Influence of stress state and temperature on secondary relaxations in polymeric glasses*

B. E. Read
Division of Materials Applications, National Physical Laboratory, Teddington, Middlesex, TW11 0LW, UK
(Received 11 February 1981; revised 3 April 1981)

Using a range of dynamic techniques, the components of the complex tensile modulus E^*, Poisson's ratio v^*, shear modulus G^* and bulk modulus K^* have been determined at 21°C in the frequency range 10^{-2} to 10^7 Hz for PMMA and rigid PVC. Some E^* data obtained for PMMA over a range of both frequency and temperature are also presented. A frequency dependence of the components of both G^* and K^* is observed throughout the broad β relaxation regions in PMMA and PVC at room temperature. The β relaxation mechanisms are discussed in relation to the calculated relaxation magnitudes, relaxation time distributions and activation energy distribution. From an analysis of dynamic mechanical and strain-birefringence data, an assessment is made of the validity of the frequency–temperature superposition procedure as applied to secondary relaxation phenomena in polymeric glasses.

INTRODUCTION

The characterization and understanding of mechanical relaxation processes in glassy polymers should benefit considerably from the availability of reliable dynamic data covering wide ranges of frequency and temperature and different types of stress field[1-5]. For purposes of illustration, we present in this paper an analysis of data obtained in the frequency range 10^{-2} to 10^7 Hz for polymethyl methacrylate (PMMA) and rigid polyvinyl chloride (PVC). From these results, estimates have been made of the magnitudes of the secondary (β) relaxations for tensile, shear and volume deformations respectively. Dynamic tensile data for PMMA have also been analysed to obtain approximate relaxation time distributions at different temperatures and subsequent assessments made of the distribution of activation energies hindering the local molecular motions. On the basis of these analyses, the validity of the frequency–temperature shift procedure for extending the effective frequency range and deriving activation energies for the β processes in PMMA is discussed.

THEORY

The results of dynamic mechanical studies are conventionally specified in terms of the components of some complex modulus M^* given by[1-8]:

$$M^* = M' + iM'' = M'(1 + i\tan\delta_M) \qquad (1)$$

where $i = (-1)^{1/2}$ and M', M'' and $\tan\delta_M$ are the respective frequency dependent storage modulus, loss modulus and damping factor. δ_M is the phase angle by which a time-harmonic stress cycle leads the strain cycle in low-frequency, low-amplitude, non-resonance tests.

The two basic types of mechanical stress field correspond to shear and to hydrostatic tension/compression and the relevant complex moduli obtained from dynamic tests on isotropic materials are the shear modulus ($M^* = G^*$) and the bulk modulus ($M^* = K^*$) respectively. In practice, however, other related moduli may be more conveniently determined for rigid polymeric glasses. Dynamic tensile tests may yield the components of the complex tensile modulus ($M^* = E^*$) and Poisson's ratio ($v^* = v' - iv'' = v'(1 - i\tan\delta_v)$) whilst the components of a longitudinal modulus ($M^* = L^*$) are obtained from the velocity and attenuation of ultrasonic waves transmitted through the polymer. For isotropic materials, the components of any one of these complex functions can, in principle, be calculated from the measured components of any two other functions at a given frequency and temperature. Approximate relationships for effecting these calculations have been given together with a discussion of the error magnifications involved[9].

Linear relaxation relationships

According to linear viscoelastic theory[1,3,6,7] M' and M'' may each be expressed as a function of frequency in terms of a normalized relaxation time distribution $\varphi_M(\log\tau)$ where $\varphi_M(\log\tau)\,\mathrm{d}\log\tau$ represents the fraction of relaxation processes having relaxation times in the range $\log\tau$ to $\log\tau + \mathrm{d}\log\tau$. Here $\log\tau$ is the logarithm to base ten and we may write:

$$M' = M_R + (M_U - M_R)\int_{-\infty}^{\infty} \varphi_M(\log\tau)\frac{\omega^2\tau^2}{1+\omega^2\tau^2}\mathrm{d}\log\tau \qquad (2)$$

$$M'' = (M_U - M_R)\int_{-\infty}^{\infty} \varphi_M(\log\tau)\frac{\omega\tau}{1+\omega^2\tau^2}\mathrm{d}\log\tau \qquad (3)$$

* Presented at the 10th Europhysics Conference on Macromolecular Physics entitled 'Structure and Motion in Polymer Glasses', Noordwijkerhout, The Netherlands, April 21-25, 1980

0032-3861/81/111580-07$02.00
©1981 IPC Business Press

where ω is the angular frequency and M_U and M_R are the limiting unrelaxed and relaxed moduli at high and low frequencies respectively. From equation (3) it follows that $M_U - M_R$ may be evaluated from the integrated area beneath a plot of M'' against log f, where the cyclic frequency f equals $\omega/2\pi$, using:

$$M_U - M_R = \frac{4.606}{\pi} \int_{-\infty}^{\infty} M'' \, \mathrm{d} \log f \tag{4}$$

Various approximate methods have been proposed[1] for evaluating the relaxation time distribution from plots of M' or M'' against log f at constant temperature. If the variations in M' and M'' occur over a very broad frequency range, as is frequently the case with secondary relaxation regions in glassy polymers, then the zeroth order approximation[1]

$$\varphi_M(\log \tau) \approx \frac{4.606\, M''}{\pi(M_U - M_R)} \text{at } \tau = 1/\omega \tag{5}$$

is often adequate and convenient.

Activation energy distributions

From equation (5) it follows that the most probable relaxation time τ_m within the distribution equals $1/2\pi f_m$ where f_m is the frequency of maximum loss modulus. Furthermore, since plots of log f_m against reciprocal absolute temperature ($1/T$) are accurately linear for most secondary relaxations in glassy polymers[2,3], we may express the temperature dependence of τ_m in the Arrhenius form:

$$\tau_m = 1/2\pi f_m = \tau_{om} \exp(E_{am}/\mathrm{R}T) \tag{6}$$

Here E_{am} is the activation energy for those processes characterized by τ_m and τ_{om} is the value of τ_m in the limit of infinite temperature. Observed values of τ_{om} around 10^{-14} s are close to the reciprocal oscillation frequencies of molecular groups[2].

If it is now assumed that each relaxation time within the distribution has an Arrhenius type temperature dependence:

$$\tau = 1/2\pi f = \tau_o \exp(E_a/\mathrm{R}T) \tag{7}$$

where E_a is the activation energy associated with relaxation time τ, then the distribution of τ values can arise from a distribution of either τ_0 or E_a or from a distribution of both τ_o and E_a. Available data on secondary relaxations in polymeric glasses suggest that the loss peaks broaden appreciably with decreasing temperature indicating that a distribution of E_a values is generally involved. Assuming that $\tau_o = \tau_{om}$ for all processes[10], then from (6) and (7) it follows that:

$$\begin{aligned} \Delta E_a = E_a - E_{am} &= 2.303\, \mathrm{R}T \log(\tau/\tau_m) \\ &= 2.303\, \mathrm{R}T \log(f_m/f) \end{aligned} \tag{8}$$

Defining a normalized distribution of activation energies $\varphi(E_a)$ such that $\varphi(E_a)\, \mathrm{d}E_a$ is the fraction of processes with activation energies in the range E_a to $E_a + \mathrm{d}E_a$, then it also follows that:

$$\varphi(E_a)\, \mathrm{d}E_a = \varphi(\log \tau) \mathrm{d} \log \tau \tag{9}$$

Equations (5), (8) and (9) then yield:

$$\varphi(E_a) = \frac{\varphi(\log \tau)}{2.303\, \mathrm{R}T} = \frac{2M''}{\pi(M_U - M_R)\mathrm{R}T} \tag{10}$$

Based on the above assumptions, equation (10) enables an assessment to be made of the range of activation energies involved in the molecular motional processes responsible for the secondary relaxations in polymeric glasses.

Frequency–temperature superposition

If each relaxation time within the distribution has the same temperature dependence and the molecular processes are therefore governed by a single activation energy then, with varying temperature, plots of $\varphi_M(\log \tau)$ *versus* log τ will shift horizontally along the log τ axis without a change of shape[3]. M'-log f and M''-log f curves covering a limited frequency range at different temperatures may then be horizontally shifted onto the curve at some reference temperature to form a reduced master curve with a greatly extended effective frequency range. This frequency–temperature superposition procedure has been extensively used on data obtained in the primary glass–rubber relaxation region where the small temperature dependence of M_U and M_R can often be neglected or accounted for by small additional vertical shifts of the experimental curves[6]. The derived horizontal shift factors can then yield information on the dependence of relaxation times on temperature or free volume[6].

Applications of the frequency–temperature superposition procedure (or the equivalent time–temperature superposition principle in the case of creep or stress relaxation data) to secondary relaxations in glassy polymers[3,11,12] have recognized the need to account for the appreciable temperature dependence of M_U and M_R. For this purpose, McCrum and Morris[11] introduced the vertical shift factors c_T and d_T defined by:

$$M_{U,T_o} = c_T M_{U,T} \qquad M_{R,T_o} = d_T M_{R,T} \tag{11}$$

where subscripts T and T_o added to M_U and M_R denote a measurement temperature and reference temperature respectively. In their studies of the β relaxation in PMMA, McCrum and Morris assumed that $c_T = d_T$ and obtained values of c_T from reported moduli measured as a function of temperature at frequencies between 10^4 and 10^5 Hz. Assuming further that each relaxation time within the distribution is displaced along the log τ axis by log a_T when the temperature changes from T_o to T it follows that:

$$M'_{T_o}(a_T \omega) = c_T M'_T(\omega) \tag{12}$$

In practice, measured values of M'_T at temperature T are first reduced to M'_{T_o} by means of the vertical shift factors c_T and a_T factors are then derived from the horizontal shifts required for superposition. An activation energy $E_a = 2.303\, \mathrm{R}\, \mathrm{d} \log a_T / \mathrm{d}(1/T)$ can be subsequently calculated from the temperature dependence of a_T. However the assumptions underlying this method are somewhat questionable and may be assessed from an analysis of dynamic data covering wide ranges of both frequency and temperature.

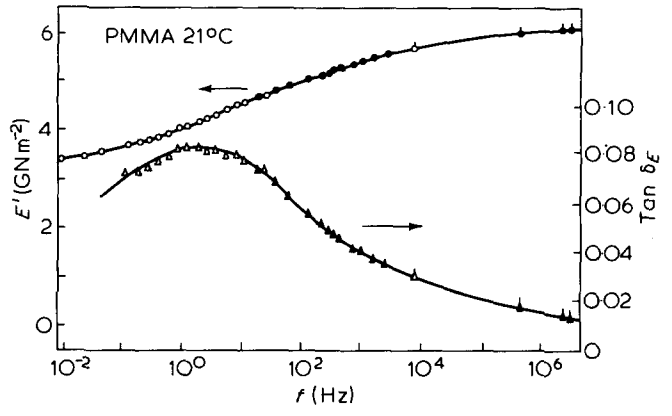

Figure 1 Variation of E' and tan δ_E with frequency for PMMA at 21°C. Point symbols as follows; ○, △, tensile forced non-resonance data; ●, ▲, flexural resonance; ◐, ◬, longitudinal resonance; ◆, ▲, ultrasonic pulse propagation

EXPERIMENTAL

In previous publications[4,9], details have been given of our range of dynamic test methods for determining the various storage moduli and damping factors in the frequency range 10^{-2} to 10^{7} Hz. Here we outline briefly the relevant frequency ranges and quantities obtainable from the different techniques for polymeric glasses.

(a) The *ultrasonic pulse method* yields directly the components of L^* and G^* at frequencies between 0.5 and 10 MHz from the velocity and attenuation of respective longitudinal and transverse waves in the material. From these measurements the components of E^*, ν^* and K^* can be evaluated to good accuracy.

(b) The *longitudinal resonance method* gives the E^* components at frequencies around 10 kHz from the measured resonance frequencies and resonance peak widths.

(c) From *torsional resonance* frequencies and associated peak widths the components of G^* are obtained at frequencies above about 500 Hz.

(d) *Flexural resonance* measurements yield the components of E^* in the frequency range 100 Hz to 10 kHz.

(e) The *torsion pendulum* provides G^* data at low frequencies (0.1 to 10 Hz) from the period and decay-rate of free torsional oscillations of samples with added inertia.

(f) The *tensile forced non-resonance* technique yields the components of E^* at frequencies between 10^{-2} and 10^{3} Hz from direct measurements of the respective amplitudes and phases of the stress and strain cycles for a polymer strip subjected to a time-harmonic deformation. If bidirectional strain gauges are bonded to the specimen surfaces, then the components of ν^* can be evaluated from the measured amplitudes and phases of the lateral and longitudinal strain cycles. The measured components of E^* and ν^* can be subsequently employed to compute the components of K^* and G^*. Since the development of the latter method is of recent origin[9,13], it is appropriate to present here the relevant relationships in full. These are as follows:

$$G' = \frac{E'}{2(1+\nu')} \cdot \frac{1-\alpha\tan\delta_E}{1+\alpha^2} \tag{13}$$

$$\tan\delta_G = \frac{\tan\delta_E+\alpha}{1-\alpha\tan\delta_E} \tag{14}$$

$$K' = \frac{E'}{3(1-2\nu')} \cdot \frac{1+\gamma\tan\delta_E}{1+\gamma^2} \tag{15}$$

$$\tan\delta_K = \frac{\tan\delta_E-\gamma}{1+\gamma\tan\delta_E} \tag{16}$$

where $\alpha = \frac{\nu'}{1+\nu'}\tan\delta_\nu$ and $\gamma = \frac{2\nu'}{1-2\nu'}\tan\delta_\nu$

Since α^2, $\alpha\tan\delta_E$, γ^2 and $\gamma\tan\delta_E$ are each usually negligible compared with unity for glassy polymers equations (13) to (16) become:

$$G' \approx \frac{E'}{2(1+\nu')}, \quad \tan\delta_G \approx \tan\delta_E + \frac{\nu'}{1+\nu'}\tan\delta_\nu \tag{17}$$

$$K' \approx \frac{E'}{3(1-2\nu')}, \quad \tan\delta_K \approx \tan\delta_E - \frac{2\nu'}{1-2\nu'}\tan\delta_\nu \tag{18}$$

Values of ν' are typically about 0.37 for polymeric glasses and from (17) and (18) it follows that errors of 1% in ν' yield contributory errors of 0.27% in G' and 3% in K'. It must, however, be noted that the errors in K' increase with increasing ν' and that the approximations (18) and the determination of K' by this method break down as ν' tends to 0.5 (i.e. for rubbery polymers).

The sources and correction of errors for each of the methods employed in this investigation have been fully discussed elsewhere[4,9].

Materials

The PMMA material used in this work was a commercial grade (ICI Perspex acrylic sheet) obtained in the form of transparent sheets having a measured density at room temperature of 1185 kg m^{-3}. The unplasticized PVC was also a transparent commercial material (Cobex) having a density of 1408 kg m^{-3} at room temperature. The thermal histories of the materials were not precisely known or controlled, but they had each been stored at room temperature prior to testing for periods exceeding 5 years.

RESULTS AND DISCUSSION

Figures 1–4 show the variation with frequency of the in-phase components and the tangents of the phase angles of E^*, ν^*, G^* and K^* respectively for PMMA at 21°C. The corrected data obtained from the different methods are in good agreement and cover a substantial portion of the

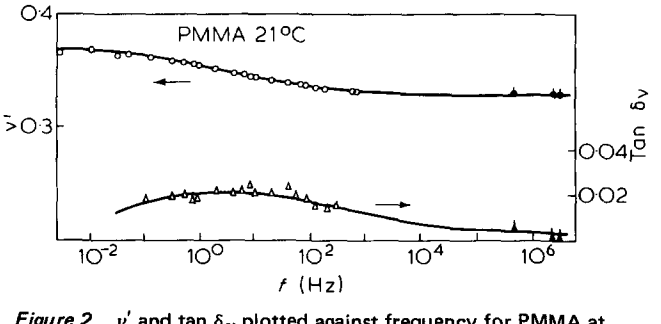

Figure 2 ν' and tan δ_ν plotted against frequency for PMMA at 21°C. Point symbols as in *Figure 1*

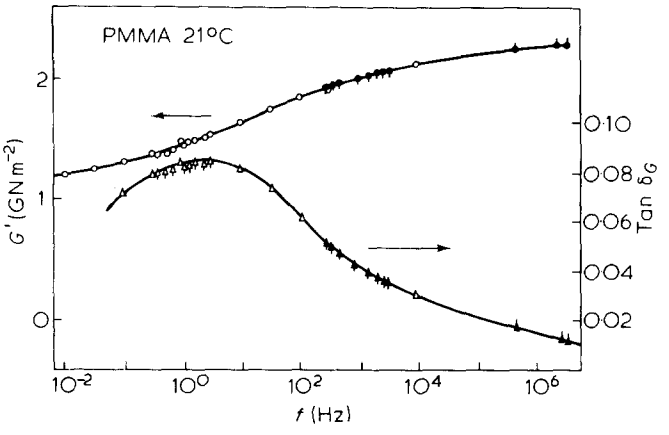

Figure 3 G' and tan δ_G *versus* frequency for PMMA at 21°C. ⚲, ⚳, torsion pendulum; ●, ▲, torsional resonance; ●, ▲, ultrasonic shear wave propagation; ○, △, calculated from E^* and ν^* tensile non-resonance results

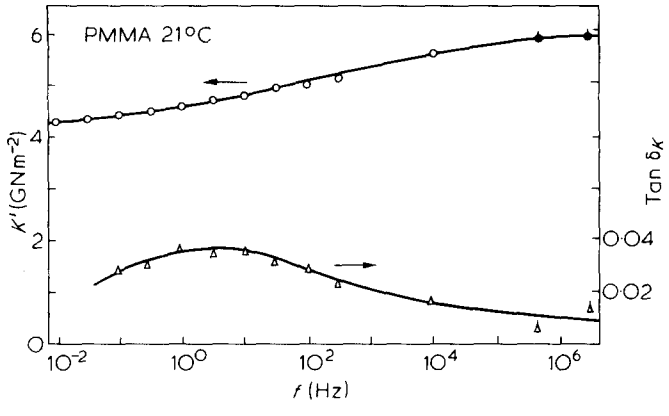

Figure 4 Variation of K' and tan δ_K with frequency for PMMA at 21°C. ●, ▲, ultrasonic data; ○, △, evaluated from E^* and ν^* results

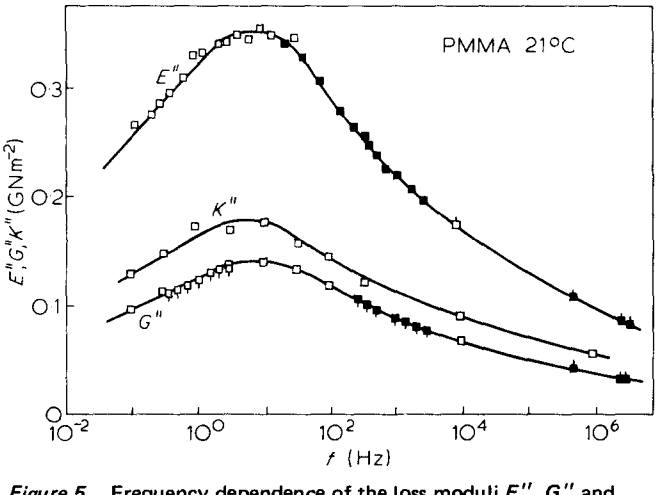

Figure 5 Frequency dependence of the loss moduli E'', G'' and K'' for PMMA at 21°C. □, From E^* and ν^* data; ■, flexural resonance; ⚐, longitudinal resonance; ⚲, torsion pendulum; ⚑, torsional resonance; ■, ultrasonic data

broad secondary β relaxation at room temperature. In particular, *Figures 3* and *4* illustrate that the components of both G^* and K^* obtained from an interpolation of E^* and ν^* results on the basis of equations (17) and (18) are frequency dependent and consistent with results obtained by other techniques. Our values of ν' are appreciably higher than those reported by Yee and Takemori[13] but the observations of relaxation effects in ν^* and K^* are consistent with the findings of these authors.

The extreme breadth of the β relaxation region in PMMA is further exemplified by the loss modulus plots in *Figure 5*. The maxima in E'', G'' and K'' occur at similar frequencies and each peak has a width of about six decades at a loss modulus level equal to half the peak value.

The variation of E' and E'' with frequency for PMMA at three temperatures is shown in *Figures 6* and *7* respectively. The plots at 60° and 100°C were constructed from a combination of our high-frequency ultrasonic data with some low-frequency results of Koppelmann[12,14]. These results illustrate the variation of relaxation magnitudes and narrowing of loss peaks with increasing temperature.

Figure 8 summarizes results obtained for rigid PVC at 21°C using our combined techniques. At frequencies between 0.1 and 200 Hz a constant ν' value of 0.37 was obtained from the tensile non-resonance method and no phase angle between the lateral and longitudinal strains could be detected. The difference between this low-frequency value and the ultrasonic ν' value of 0.36 is small

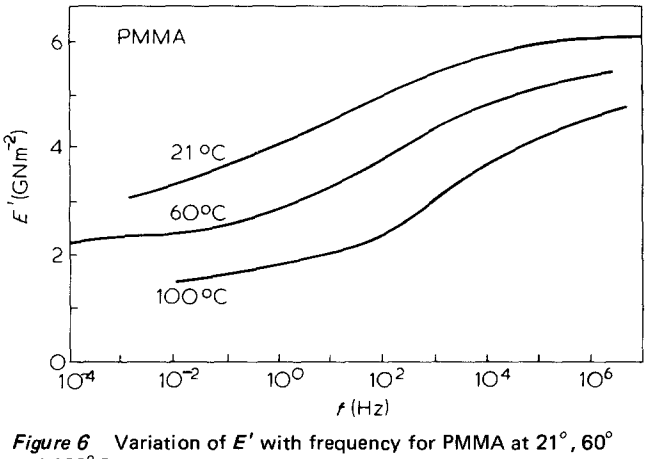

Figure 6 Variation of E' with frequency for PMMA at 21°, 60° and 100°C

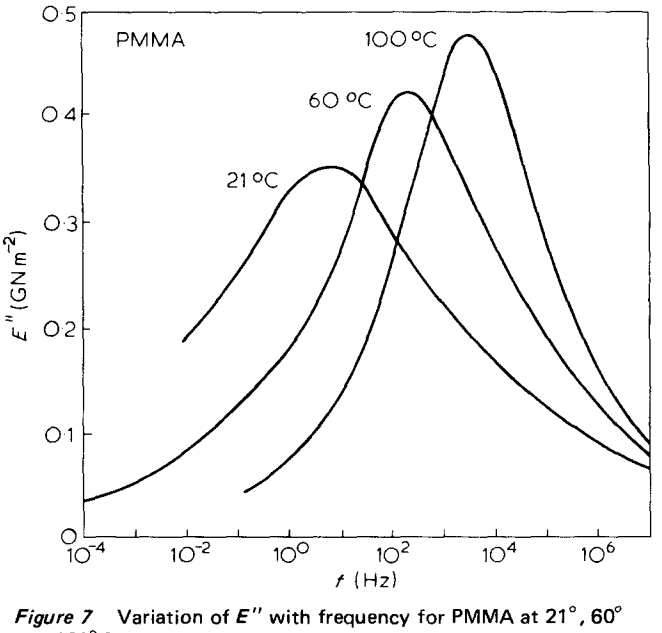

Figure 7 Variation of E'' with frequency for PMMA at 21°, 60° and 100°C

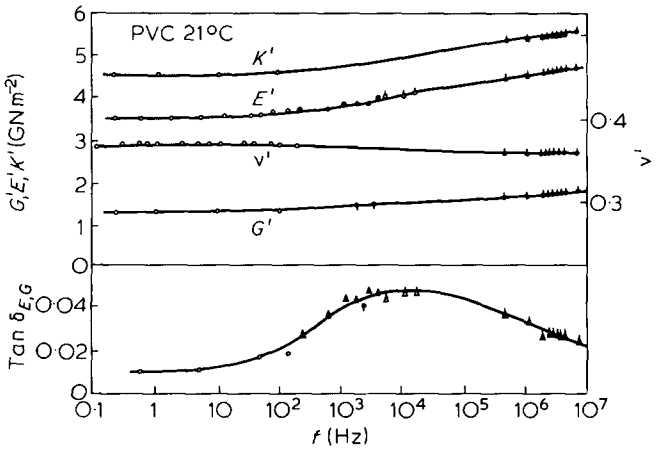

Figure 8 Summary of dynamic results for rigid PVC at 21°C. Point symbols as in *Figures 1, 2, 3* and *4*

Table 1 Modulus increments and limiting moduli for the β relaxations in PMMA and PVC

	PVC	PMMA		
	21°C	21°C	60°C	100°C
*$E_U - E_R$	1.30	3.68	3.36	2.97
E_U	4.90	6.26	5.68	4.89
E_R	3.60	2.58	2.32	1.91
$(E_U - E_R)/E_U$	0.27	0.59	0.59	0.61
$(E_U - E_R)/(E_U E_R)^{1/2}$	0.31	0.92	0.93	0.97
$G_U - G_R$	0.50	1.42		
G_U	1.80	2.34		
G_R	1.30	0.93		
$(G_U - G_R)/G_U$	0.28	0.60		
$(G_U - G_R)/(G_U G_R)^{1/2}$	0.33	0.96		
$K_U - K_R$	1.25	2.1		
K_U	5.8	5.9		
K_R	4.6	3.8		
$(K_U - K_R)/K_U$	0.22	0.35		
$(K_U - K_R)/(K_U K_R)^{1/2}$	0.24	0.44		

* Moduli in units of GN m^{-2}

and probably within the combined error of the two techniques. Values of G', tan δ_G and K' calculated from an interpolation of E^* and ν^* results are consistent with the higher frequency results. The broad frequency dispersions in E', G' and K' and the peak in tan δ_E and tan δ_G centred at frequencies above 10^4 Hz each reflect the β relaxation in PVC.

Relaxation magnitudes and relaxation time distributions

Values of $M_U - M_R$ have been computed from the integrated areas under the different loss modulus $-\log f$ plots after extrapolating the loss modulus values to zero at high and low frequencies. These calculations were based on equation (4) and the results are presented in *Table 1*. Also included in this *Table* are estimates of M_U and M_R calculated from the $M_U - M_R$ values and from values of $(M_U + M_R)/2$ assumed to equal the measured M' at the frequencies of maximum M''.

In the case of PMMA it will be observed that E_U, E_R and $E_U - E_R$ each decrease substantially with increasing temperature as is evident from *Figure 6*. However *Table 1* also illustrates that the fractional modulus increments such as $(E_U - E_R)/E_U$ and $(E_U - E_R)/(E_U E_R)^{1/2}$ are essentially independent of temperature for PMMA within the range investigated. If we thus represent the β relaxation magnitudes in terms of such fractional modulus increments, it will be observed that the ratio of bulk modulus to shear modulus relaxation magnitudes is around 0.75 for PVC and 0.5 for PMMA. Since the β relaxation must arise from local main-chain motions in PVC, and may involve closely coupled local main-chain and side group motions in PMMA, this result indicates that dilatational stress fields may interact more strongly with the main-chain than with the side group parts of the motion. This conclusion is similar to that obtained in connection with the long-range motions in the primary glass–rubber relaxation region[5] and, if confirmed, could be relevant to Heijboer's observation[15] that the fracture toughness of glassy polymers is apparently influenced by secondary main-chain motions but not by side-group motions.

Figure 9 presents the normalized relaxation time distributions for PMMA calculated from the E'' plots in *Figure 7* according to equation (5) with $M = E$. We may note that the use of a higher order approximation, involving second derivatives of the loss modulus plots[1], produced only a 3% increase in the calculated $\varphi_E(\log \tau)$ in the close vicinity of the maxima. Owing to the extreme breadth of the secondary loss peaks, equation (5) thus provides an adequate approximation with the PMMA data. The similarity in breadth and location of the E'', G'' and K'' curves for PMMA (*Figure 5*) also implies, together with equation (5), that the normalized tensile, shear and bulk modulus relaxation spectra at room temperature are similar.

Activation energy distribution

With increasing temperature, the shift in the *peak* of the $\varphi_E(\log \tau)$ to shorter relaxation times gives, according to equation (6), a most probable activation energy E_{am} of $\sim$74 kJ mol^{-1} (17.5 kcal mol^{-1}). This value is consistent with data reported in the literature[3]. Furthermore, the marked narrowing of the $\varphi_E(\log \tau)$ curves with increasing temperature suggests that the distribution of relaxation times arises predominantly from a distribution of activation energies. Assuming that $\tau_o = \tau_{om}$ for all processes (equations (6) and (7)), then a normalized distribution of activation energies, $\varphi(E_a)$ *versus* ΔE_a, has been calculated using equations (8) and (10) from the data

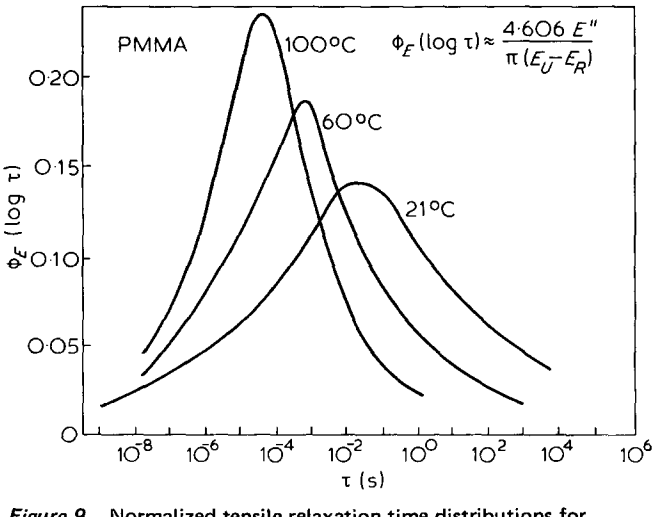

Figure 9 Normalized tensile relaxation time distributions for PMMA at 21°, 60° and 100°C

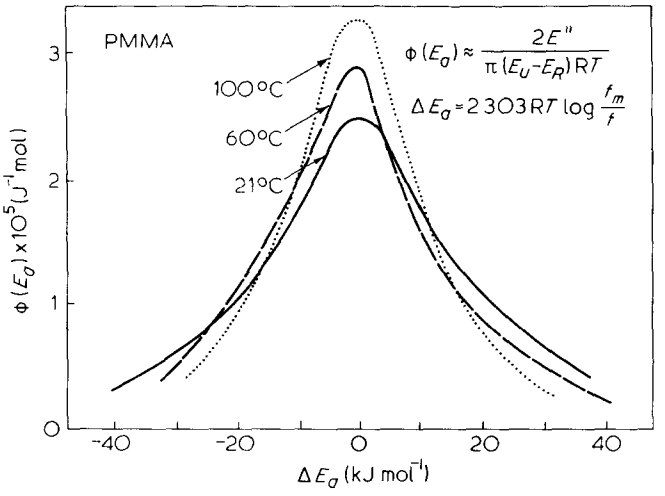

Figure 10 Normalized activation energy distributions calculated from the data for PMMA at 21°, 60° and 100°C

at each temperature. The resulting distributions (*Figure 10*) indicate that the activation energies are spread about the mean value by about ±40 kJ mol^{-1} (±10 kcal mol^{-1}). This result could arise from the range of local barriers or environments which hinder the molecular rearrangements. However the narrowing of the $\varphi(E_a)$ peaks with increasing temperature suggests that the assumptions of our model may not be strictly valid and that the loss peaks are narrowing more rapidly with increasing temperature than is implied in the assumption $\tau_o = \tau_{om}$. This could be due to the volume increase with increasing temperature which is known to produce a narrowing of loss peaks greater than that found in constant volume experiments and which is indicative of both intramolecular and intermolecular contributions to the potential barriers[16].

Frequency–temperature superposition

The observation in *Table 1* that $(E_U - E_R)/E_U$ is essentially independent of temperature for PMMA implies that $1-(c_T/d_T)(E_R/E_U)_{T_o}$, and hence that c_T/d_T, is independent of temperature. Since $c_T = d_T = 1$ at temperature T_o (equation (11)) it follows that $c_T = d_T$ at other temperatures in accordance with the hypothesis of McCrum and Morris[11]. It should perhaps be remarked that the approximately parallel appearance of the curves in *Figure 6*, which would seem to indicate that E_U and E_R have different temperature dependences, is misleading. The narrowing of the β region with increasing temperature is somewhat obscured by the increasing effects of overlap from the α relaxation on the low-frequency modulus data. At 21°C, the value of E_R is not attained at the lowest measurement frequency whereas at 100°C the E_R value is attained at a frequency around 1 Hz, the subsequent decrease in E' with decreasing frequency arising from the significant overlap of the α region. The methods for estimating E_U and E_R in this work are considered to achieve an effective resolution of the β relaxation and eliminate the overlap problem.

As mentioned earlier, the values of c_T reported by McCrum and Morris were obtained from modulus measurements at frequencies between 10^4 and 10^5 Hz. Since these frequencies lie within the broad β relaxation region at room temperature (*Figure 1*) we have reevaluated the c_T values for $T_o = 20$°C from our ultrasonic moduli determined over a wide temperature range at 2.5 MHz. It should be noted that the new c_T values, shown in *Table 2*, differ significantly from the earlier values[3,11].

On the basis of our c_T values, some earlier published E'-log f data[17] have been reduced according to equation (12) to yield E'_{T_o} *versus* log f plots with $T_o = 20$°C (*Figure 11*). Despite the rather limited accuracy of the reduced data, the master curve obtained from a subsequent horizontal superposition compares reasonably well with the directly measured curve of *Figure 1* indicated by the broken line in *Figure 12*.

A plot of the derived horizontal shift factors log a_T against $1/T$ exhibits appreciable curvature, as shown in *Figure 13*. Furthermore, at temperatures between about

Table 2 Vertical shift factors c_T for PMMA

Temperature (°C)	c_T from data at 2.5 MHz
−100	0.850
− 80	0.860
− 60	0.873
− 40	0.893
− 20	0.919
0	0.955
20	1.000
40	1.053
60	1.115
80	1.190
100	1.270

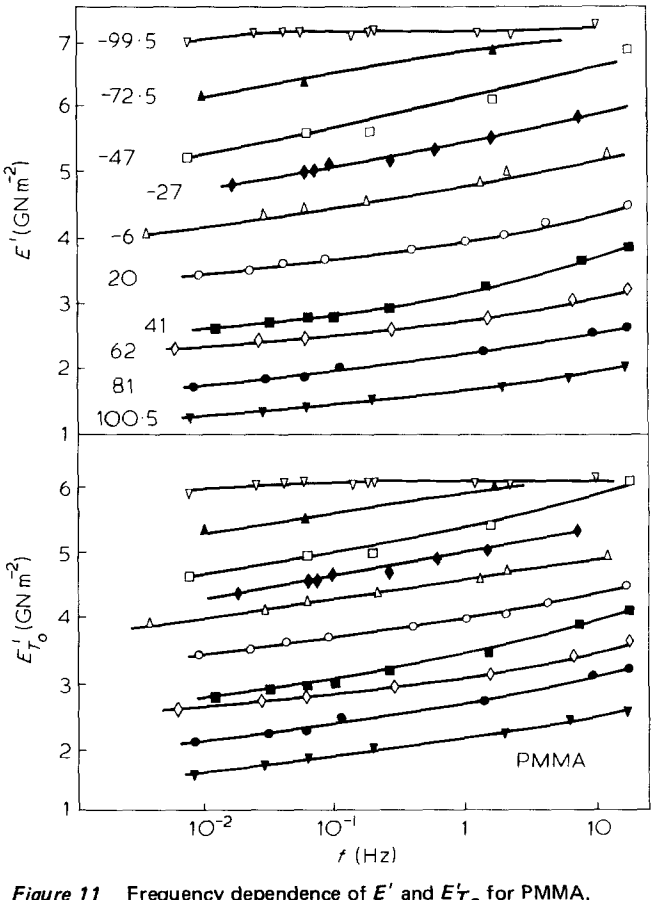

Figure 11 Frequency dependence of E' and E'_{T_o} for PMMA. The reference temperature T_o = 20°C and different point symbols refer to different temperatures of measurement (°C) as indicated on the E' curves

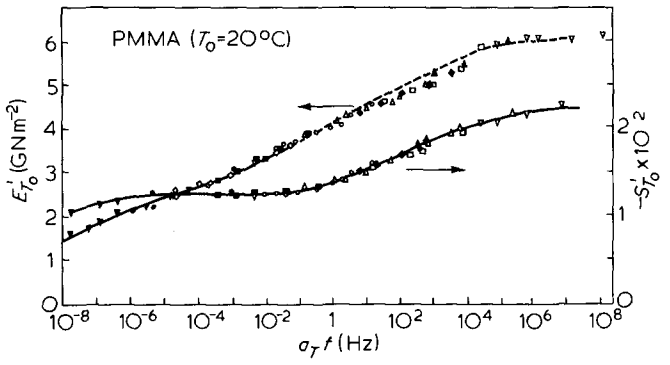

Figure 12 Master curves of E'_{T_0} and the in-phase strain-optical coefficient S'_{T_0} for PMMA. The reference temperature T_0 = 20° C. (– – –), directly measured curve from *Figure 1*. Point symbols as in *Figure 11*

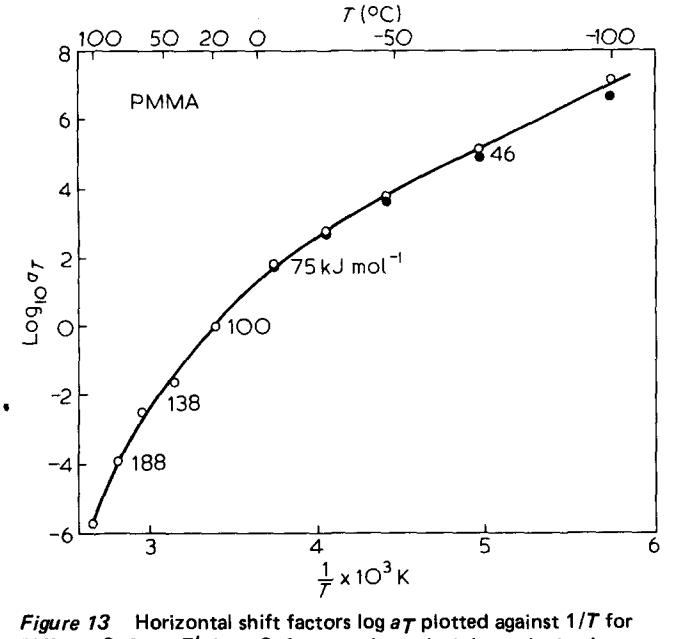

Figure 13 Horizontal shift factors log a_T plotted against $1/T$ for PMMA. ○, from E' data; ●, from strain-optical data. Activation energies derived from slopes at different temperatures are indicated

+50 and −100°C the activation energies estimated from the slopes of this curve are within the range indicated in *Figure 10*. It is important to emphasize that the observed curvature does not imply a temperature dependent apparent activation energy since a plot of log τ_m against $1/T$ is strictly linear according to equation (6). We conclude that the curvature arises from a distribution of activation energies and that the assumption of a single activation energy which underlies the frequency–temperature superposition principle is invalid in the case of the β relaxation in PMMA.

Also included in *Figures 12* and *13* are the results of applying the frequency–temperature superposition principle to the in-phase component of the complex strain-optical coefficient[17] $S^*=S'+iS''$. It should be noted here that the a_T factors derived from the optical data are in good agreement with the mechanical a_T values and were obtained without the application of any vertical shift factors. The latter observation is consistent with the recent suggestion[18] that the equilibrium strain-optical coefficient in glassy PMMA should be almost independent of temperature. *Figure 12* also illustrates that the β strain-optical relaxation region in PMMA reflects the higher frequency motions responsible for the broad mechanical relaxation time distribution.

Some final comments should be made concerning the possible effects of thermal history on the results presented here. Although the glassy materials will not have attained volume equilibrium, the periods of storage at room temperature should have ensured that they had physically aged to an effectively stable free-volume with respect to the subsequent duration of testing at room temperature and below. In fact the room temperature data in *Figures 1–5* and in *Figure 8* were found to be reproducible over the period of about 1 year during which the measurements were made. It should also be emphasized that all data were obtained at frequencies and temperatures corresponding predominantly to the β relaxations for each material. According to Struik[19], the principal effect of physical ageing is to increase the (free-volume dependent) relaxation times associated with the primary or α glass–rubber relaxation processes and the β processes are relatively little affected. At room temperature and below, the β regions for both PMMA and PVC (observed with varying frequency at constant temperature) are fairly well resolved from the respective α regions and may not therefore be substantially influenced by thermal history. The data for PMMA at temperatures above 60°C and at the lower frequencies could, however, be more sensitive to ageing through partial overlap of the α and β regions. For the above reasons we would not anticipate a marked influence of thermal history on the results presented here but future systematic studies of physical ageing effects are envisaged.

REFERENCES

1 Staverman, A. J. and Schwarzl, F. in 'Die Physik der Hochpolymeren' (Ed. H. A. Stuart) Springer–Verlag, Berlin, 1956, Vol 4, Ch 1
2 Heijboer, J. *Int. J. Polym. Mater.* 1977, **6**, 11
3 McCrum, N. G., Read, B. E. and Williams, G. 'Anelastic and Dielectric Effects in Polymeric Solids', Wiley, London and New York, 1967
4 Read, B. E. and Dean, G. D. 'The Determination of Dynamic Properties of Polymers and Composites', Adam Hilger Ltd., Bristol, 1978
5 Marvin, R. S. and McKinney, J. E. *Phys. Acoust.* 1965, **2B**, 165
6 Ferry, J. D. 'Viscoelastic Properties of Polymers', Wiley, New York, 1961
7 Ward, I. M. 'Mechanical Properties of Solid Polymers', Wiley–Interscience, London, 1971
8 Plazek, D. J. *Meth. Exp. Phys.* 1980, **16C**, 1
9 Read, B. E. and Duncan, J. C. 'Polymer Testing', Applied Science Publishers, 1981, **2**, 135
10 Kolarik, J. *Coll. Czech. Chem. Commun.* 1971, **36**, 2049
11 McCrum, N. G. and Morris, E. L. *Proc. Roy. Soc., A*, 1964, **281**, 258
12 Koppelmann, J., Leder, H. and Royer, F. *Colloid Polym. Sci.* 1979, **257**, 673
13 Yee, A. F. and Takemori, M. T. *ACS Polym. Prepr.* April 1979, **20**, No 1, 758
14 Koppelmann, J. and Hirnböck, R. *Polym. Eng. Sci.* 1978, **18**, 1087
15 Heijboer, J. *J. Polym. Sci.* 1968, **C16**, 3755
16 Koppelmann, J. *Progr. Coll. Polym. Sci.* 1979, **66**, 235
17 Read, B. E. *J. Polym. Sci.* 1967, **C16**, 1887
18 Pick, M. and Lovell, R. *Polymer* 1979, **20**, 1448
19 Struik, L. C. E. *Polym. Eng. Sci.* 1977, **17**, 165